AD-A020 723

LASER DAMAGE IN 8- TO 14-MICRON MERCURY-CADMIUM-
TELLURIDE PHOTOVOLTAIC DETECTOR MATERIAL

F. Bartoli, et al

Naval Research Laboratory

Prepared for:
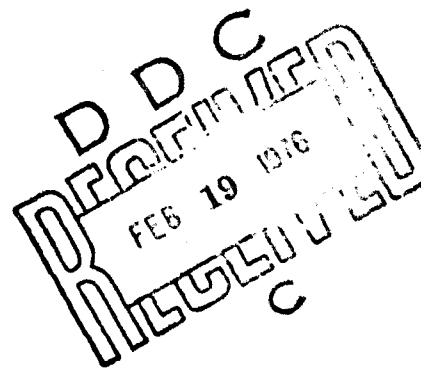
Advanced Research Projects Agency

20 January 1976

055055

Laser Damage in 8- to 14-Micron Mercury-Cadmium-Telluride Photovoltaic Detector Material

F. Bartoli, L. Esterowitz, R. Allen and M. Kruer

Optical Warfare Branch
Optical Sciences Division

January 20, 1976

NAVAL RESEARCH LABORATORY
Washington, D.C.

REPORT DOCUMENTATION PAGE		READ INSTRUCTIONS BEFORE COMPLETING FORM
1 REPORT NUMBER NRL Report 7959	2 GOVT ACCESSION NO.	3 RECIPIENT'S CATALOG NUMBER
4 TITLE (and Subtitle) LASER DAMAGE IN 8- TO 14-MICRON MERCURY-CADMIUM-TELLURIDE PHOTOVOLTAIC DETECTOR MATERIAL		5 TYPE OF REPORT & PERIOD COVERED Interim report on a continuing NRL Problem.
		6 PERFORMING ORG. REPORT NUMBER
7 AUTHOR(s) F. Bartoli, L. Esterowitz, R. Allen, and M. Kruer		8 CONTRACT OR GRANT NUMBER(s)
9 PERFORMING ORGANIZATION NAME AND ADDRESS Naval Research Laboratory Washington, D.C. 20375		10 PROGRAM ELEMENT, PROJECT, TASK AREA & WORK UNIT NUMBERS NRL Problem N01-36.501 ARPA Order 2274
11 CONTROLLING OFFICE NAME AND ADDRESS Advanced Research Project Agency 1400 Wilson Boulevard Arlington, Virginia 22209		12 REPORT DATE January 20, 1976
		13 NUMBER OF PAGES 14
14 MONITORING AGENCY NAME & ADDRESS(if different from Controlling Office)		15 SECURITY CLASS. (of this report) Unclassified
		15a DECLASSIFICATION DOWNGRADING SCHEDULE
16 DISTRIBUTION STATEMENT (of this Report) Approved for public release: distribution unlimited.		
17 DISTRIBUTION STATEMENT (of the abstract entered in Block 20, if different from Report)		
18 SUPPLEMENTARY NOTES		
19 KEY WORDS (Continue on reverse side if necessary and identify by block number) HgCdTe photovoltaic detectors Laser damage Detector thermal modeling Finite-element calculations		

20 ABSTRACT (Continue on reverse side if necessary and identify by block number)

   A two-dimensional thermal analysis of laser-irradiated HgCdTe photovoltaic (PV) detectors is presented, and irreversible damage thresholds are determined as a function of irradiation time and beam diameter. Damage thresholds were measured experimentally for HgCdTe crystals similar in size and mounting to those used in operating photovoltaic detectors. Calculated thresholds for HgCdTe PV detectors are compared to those for HgCdTe photoconductive (PC) and PbSnTe PV detectors.
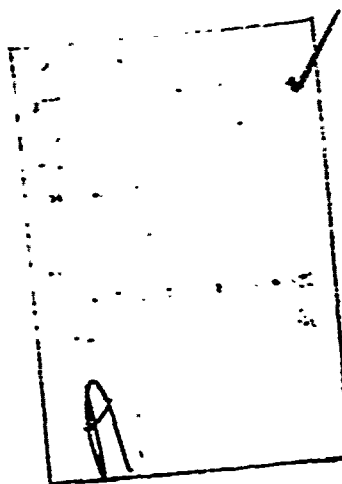
DD FORM 1473 EDITION OF 1 NOV 65 IS OBSOLETE
S N 0102-014-6601

CONTENTS

LASER DAMAGE IN 8- TO 14-MICRON MERCURY-CADMIUM-TELLURIDE PHOTOVOLTAIC DETECTOR MATERIAL

INTRODUCTION

Mercury-cadmium telluride photovoltaic (PV) detectors are of particular importance for detection of radiation in the 8-to 14-μm spectral region, where high responsivity and very fast response times are required. In this report 10.6-μm laser damage in HgCdTe is studied both experimentally and theoretically. Damage thresholds of HgCdTe crystals, similar in geometry to those used for photovoltaic detectors, were measured, and their dependence on irradiation time was studied. A thermal model was used to predict damage thresholds for $Hg_{0.8}Cd_{0.2}Te$ P.V detectors, and these results are compared to experimental values. Effects of laser beam diameter and detector thermal configuration are discussed. Damage thresholds for this detector are compared to those for other 8 to 14-μm detectors.

In what follows we assume that the material properties are independent of temperature and may be treated as constants. The detector is assumed to be initially at a reference temperature T_{ref}. Nonlinear effects as well as variations in material properties with optical flux are neglected. It is assumed that no phase change is required for junction degradation and that the damage threshold refers to the irradiation level required to raise the temperature of the detector surface to some critical temperature T_{tr}. The absorbed energy either raises the temperature of the absorbing volume or is conducted away toward the heat sink.

THEORY

In a previous work [1] it was concluded that a thermal model for a semi-infinite solid irradiated by a Gaussian beam can be used to predict damage thresholds for photovoltaic detectors as long as the beam diameter is small compared to both detector thickness and width. A cross-sectional view of a typical photovoltaic detector (Fig. 1) illustrates Gaussian beam irradiation of a detector with finite thickness and sample area. The power density profile of a Gaussian beam is given by $P(r) - Pe^{-r^2 k^2}$, where P is the flux (W/cm^2) at the center of the beam. The temperature profile in a semi-infinite material with an infinite absorption coefficient, heated at the surface by this Gaussian beam, is [2]

$$\Delta T(r, z, \tau) = \frac{(1 - R)Pa^2}{\rho c \sqrt{\pi k}} \int_0^\tau \frac{dt}{\sqrt{t(4kt + a^2)}} \exp\left[-\frac{z^2}{4kt} - \frac{r^2}{4kt + a^2} \right]. \quad (1)$$

where R is the reflectivity, ρ is the density, c is the specific heat, k is the thermal diffusivity, and τ is the irradiation time. The temperature change at the surface of the material ($z = 0$) and at the center of the beam ($r = 0$) is
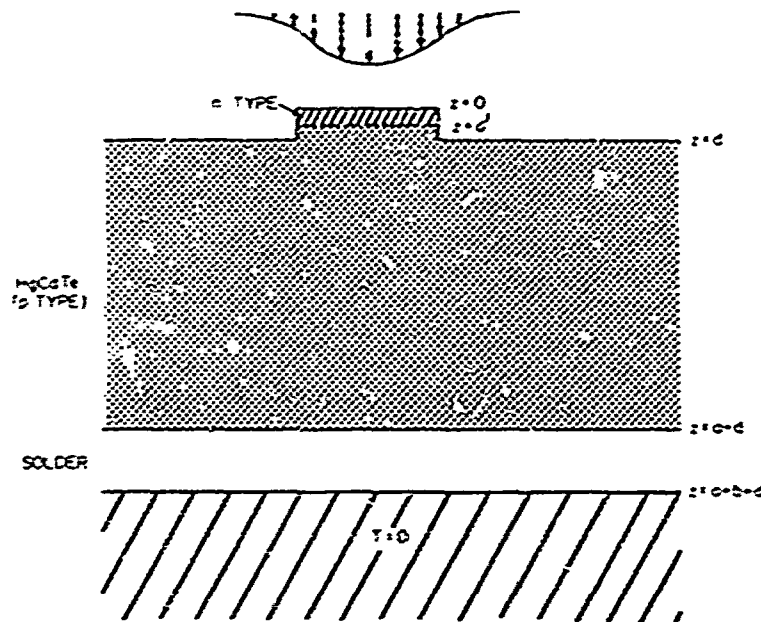
Fig. 1 — Cross-sectional diagram of a typical HgCdTe (PV) detector

$$\Delta T(0, 0, \tau) = \frac{(1 - R) P_0}{\rho c k \sqrt{\pi}} \cdot \tan^{-1} \left(\frac{4k\tau}{a^2}\right)^{1/2} . \tag{2}$$

Equation (2) can be solved to give the power density P_0 and energy density $E_0 = P_0\tau$ required to change the temperature of the surface by $\Delta T_{th} = T_{th} - T_{ref}$. However, since actual detectors have a finite absorption coefficient, Eq. (2) is valid only at long times, when the heat diffuses distances much greater than the absorbtion depth $1/a$. This model was modified in Ref. 1 to take into account the finite absorption coefficient. It was shown that an approximate expression for E_0 is given by

$$E_0 = \frac{\Delta T_{th}\rho c}{(1 - R)a} \left[1 + \frac{k\tau a}{a \tan^{-1} \left(\frac{4k\tau}{a^2}\right)^{1/2}} \right] . \tag{3}$$

The first term in this expression is dominant at short times, when thermal conduction is not important and the temperature change is determined by the depth over which the heat is absorbed. The second term is dominant at long times, when the heat-diffusion depth $\sqrt{k\tau}$ is much greater than the absorption depth $1/a$.

2

For detectors whose thickness is less than or equal to the beam diameter, Eq. (3) may result in considerable error. For such detectors a more elaborate thermal model, taking into account both laser beam diameter and relevant details of detector geometry, is required for an accurate theoretical determination of damage thresholds. In the present work we apply such a model, based on a numerical technique, to HgCdTe PV detectors. Damage thresholds are calculated for two beam diameters, one less than and one greater than the detector thickness. These results illustrate the importance of the more sophisticated numerical model in predicting damage thresholds for such experimental conditions.

There are several methods for numerically evaluating transient temperature distributions in heated materials. Among these are finite-difference methods, variational methods, and finite-element methods. For our work we chose a finite-element method developed by Torvik [3] which differs from the more traditional finite-element methods in the technique used for evaluation. The approach taken was to divide the region of interest into a large number of finite segments and to perform a heat balance on each. For the same number of elements this method is expected to be less accurate than the traditional finite-element method, but it is expected to be more practical for many aspects of thermal modeling in detectors. The accuracy of this method was examined by Torvik. For our calculations periodic checks on the accuracy were performed by comparing the results of the computer program with the results of exact closed-form solutions. The element sizes were chosen to be sufficiently small that the difference between the numerical model and the closed-form solutions was always less than 3 percent.

The geometry considered is a circular plate or disk consisting of two slabs having different material properties. These slabs correspond to the detector and substrate. The laser flux is incident on the front surface and is absorbed exponentially below the surface. The boundary conditions on the edges and rear surface are chosen to correspond to the experimental environment of the detector. The thickness of the disk b is divided into N_P layers of thickness ΔZ. The radius is divided into N_C segments of width ΔR. It is assumed that the material is heated by an axially symmetric flux. Hence no azimuthal subdivision is required.

The disk is divided into $N_C \times N_P$ elements each having the form of a solid annulus. The rate of heat flow through the i, j element is given by the product of the conductivity $K_{i,j}$, the area of the interface, and the temperature gradient in the direction of heat flow. For example, the rate at which heat flows through an area $A_{z_{i,j}}$ from the i, j element, due to a temperature gradient in the z direction, is

$$Q_{z_{i,j}} = K_{z_{i,j}} A_{z_{i,j}} \left[\frac{T_{i,j} - T_{i+1,j}}{\Delta Z_{i,j}} \right]. \tag{4}$$

where $T_{i,j}$ and $T_{i+1,j}$ are the temperatures of the i, j and $i+1, j$ elements respectively. The rate of radial heat flow $Q_{R_{i,j}}$ is defined analogously. Heat can also enter the element by absorption from external sources (e. g., optical radiation). We must add to the heat-balance equation an additional term $P_{i,j}$ (watts) which is the rate at which heat is added externally to the i, j element. It is assumed that phase changes or internal reactions do not occur. The net rate of energy flow in the i, j element is depicted schematically in Fig. 2.
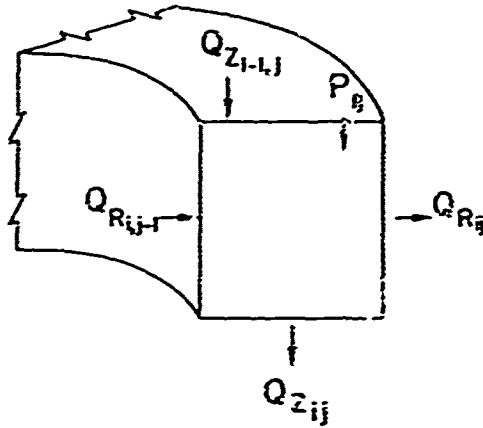
3

Fig. 2 - Schematic representation of energy flow in the ij element

The net flow energy ΔQ_{ij} is given by

$$\Delta Q_{ij} = P_{ij} + Q_{R_{i,j-1}} + Q_{Z_{i-1,j}} - Q_{R_{ij}} - Q_{Z_{ij}},$$ (5)

and the temperature change ΔT_{ij} is

$$\Delta T_{ij} = \frac{\Delta Q_{ij} \Delta t}{c_{ij} m_{ij}},$$ (6)

where Δt is the time increment, c_{ij} is the specific heat, and m_{ij} is the mass. The preceding heat balance is performed repeatedly using a small time increment Δt until the sum of the time increments equals the time of interest. At each time step the temperature change ΔT_{ij} in the ij element is added to the previous temperature T_{ij}. The temperature for an irradiation time $\tau = n\Delta t$ (n time intervals) can be written

$$T_{ij}(\tau) = T_{ref} + \sum_{k=1}^{n} \Delta T_{ij}(k),$$ (7)

Where $\Delta T_{ij}(k)$ is the temperature change calculated for the kth time interval.

To calculate the threshold for damage on the surface at the center of the Gaussian beam, we consider $T_{1,1}(\tau)$. To express damage thresholds in terms of quantities calculated by the model, we introduce a normalized temperature increase for the 1,1 element: $\Delta\theta(\tau) = [T_{1,1}(\tau) - T_{ref}]/P$. Here $P \approx P_{1,1}/A_{z_{1,1}}$ since $\Delta R_{1,1}$ is always small compared to the beam radius a. Assuming damage occurs when the temperature increase $[T_{1,1}(\tau) - T_{ref}]$ is equal

4

to ΔT_{th}, the power-density threshold P_0 can be written as $P_0 = \Delta T_{th}/\Delta\theta(\tau)$. Therefore threshold levels of laser energy density E, in terms of ΔT_{th} and $\Delta\theta$ are simply given by

$$E_0 = \frac{\Delta T_{th}\tau}{\Delta\theta(\tau)}. \tag{8}$$

RESULTS

The $Hg_{0.8}Cd_{0.2}Te$ materials were irradiated with 10.6-μm laser pulses with irradiation times varying from 1 μs to approximately 1 s. Values of power density ranged from 10^3 to 10^6 W/cm^2, and pulse energy densities ranged from 1 to 10^4 J/cm^2. The experimental apparatus and procedure is discussed in detail elsewhere [2]. A 1-mm square p-type crystal approximately 0.5 mm thick was bonded to a gold-plated copper mount (2 mm thick) which was in contact with a copper cold finger held at 77°K. The surface of the sample was polished and then etched with a 5% bromine in methyl alcohol. The optical, mechanical, and thermal properties of these samples are expected to be roughly the same a for operating photovoltaic detectors.

Threshold values of peak energy density E_0 and peak power density P_0 for material damage are presented in Table 1. Measurements over six orders of magnitude variation in irradiation time were made using a laser beam whose full width at half maximum (FWHM) was 0.25 mm. Damage thresholds were also obtained using a beam (FWHM = 1.0 mm) which covered the entire crystal, thus approximating uniform irradiation conditions. For this large beam diameter, radial heat conduction is not expected to significantly affect the damage thresholds. Note that both E_0 and P_0 vary by approximately three orders of magnitude over the range of irradiation times studied. Uncertainty in the damage threshold is estimated at 30 to 40 percent.

Table 1
Damage Thresholds For $Hg_{0.8}Cd_{0.2}Te$ Material

FWHM (mm)	τ (s)	E_0 (J/cm^2)	P_0 (kW/cm^2)
0.25	1×10^{-6}	2.2	2200
0.25	3×10^{-4}	8.0	26.7
0.25	4.4×10^{-2}	400	9.1
0.25	8×10^{-1}	4500	5.6
1.0	8×10^{-3}	29	3.6
1.0	2×10^{-1}	330	1.65

When the temperature rise at the crystal surface reaches a threshold value ΔT_{th}, damage will occur. Since thermal decomposition and the resulting outgasing of mercury are rate

processes, ΔT_{th} will have some dependence on irradiation time. In the numerical model discussed previously, however, ΔT_{th} was assumed to be constant. Due to the complicated time- and power-dependent nonequilibrium dynamics (decomposition and vaporization) taking place on such short time scales, ΔT_{th} is not a known quantity and is therefore determined empirically in fitting the data. The thermal conductivity K of HgCdTe varies considerably over the temperature range of interest. However, values of K are not known over this entire range, and it is impossible to determine a priori a "suitably averaged" value of thermal conductivity. Therefore K was also determined by treating it is an adjustable parameter in fitting the data. E_0 is approximately independent of K for short irradiation times, where the thermal diffusion distance is small compared to the absorption depth. ΔT_{th} was obtained by fitting this short-time data ($\tau \approx 1\ \mu s$). Then using this value of ΔT_{th}, K was determined by fitting the data for longer irradiation times. Although the absorption coefficient α also varies strongly with temperature, a "suitably averaged" value of this parameter has been obtained in a previous study [1]. This same value ($\alpha = 10^3\ cm^{-1}$) was used here.

Using published values of HgCdTe material parameters (Table 2), the numerical thermal model discussed in the preceding was used to calculate E_0 and P_0 as a function of irradiation time. These results are plotted in Figs. 3 and 4 together with the experimental data. We note that for both beam diameters studied the theoretical model for detector damage is in good agreement with the experimental results on HgCdTe material samples. The calculated damage thresholds for HgCdTe (PV) detectors exhibit three distinct regions of behavior. For short irradiation times, E_0 is constant, and P_0 is inversely proportional to τ, whereas for intermediate times, $E_0 \propto \tau^{1/2}$, and $P_0 \propto \tau^{-1/2}$. In the long-time limit, P_0 asymptotically approaches a constant value. The thresholds obtained using the Gaussian beam (FWHM = 0.25 mm) is nearly an order of magnitude greater than for "uniform irradiation" in the long-time-limit. For the Gaussian beam the values of E_0 and P_0 at long times are determined mainly by radial heat conduction. For uniform irradiation, radial heat conduction is unimportant, and the thresholds are limited by the finite sample thickness and the thermal coupling with the heat sink [1].

Table 2
Properties Of $Hg_{0.8}Cd_{0.2}Te$

Thermal diffusivity k:	$0.09\ cm^2/sec$ at $77°K$*
Thermal conductivity K:	$0.10\ W/cm\ °K$*
Density ρ:	$7.6\ gm/cm^3$*
Reflectivity R:	0.31*
Specific heat c:	$0.15\ J/gm\ °K$‡
Absorption coefficient α:	$10^3\ cm^{-1}$‡
ΔT_{th}:	$660°K$§
Threshold temperature increase	

*D. Long and J. L. Schmit, Semiconductors and Semimetals 5, Ch. 6, R. K. Willardson and A. C. Beer, editors, Academic Press, New York 1970. Value of k and K obtained empirically from the fit of damage threshold data, refer to values suitably averaged over the temperature range of interest.

‡ Extrapolated from data in P. Goldfinger and M. Jeunehomme, Trans. Faraday Soc. 59, 2851 (1963).

‡ The absorption coefficient is assumed to be the same as used earlier for HgCdTe PC detectors. (See Ref. 1.)

§ Our results indicate that without an antireflection (AR) coating, HgCdTe requires approximately a 0.67 times smaller temperature increase for vaporization than for the AR-coated PC detector. The temperature rise obtained earlier for HgCdTe (PC) is 950°K, giving $\Delta T_{th} = 660°K$ for the uncoated HgCdTe PV detector.
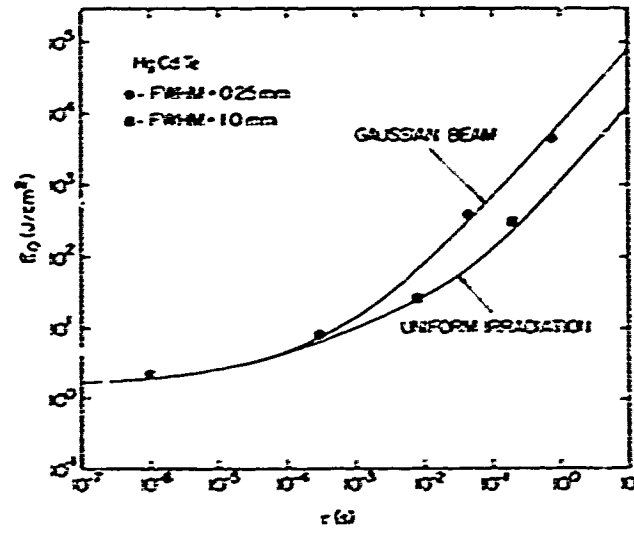
6

Fig. 3 — Energy-density damage thresholds for
HgCdTe crystals as a function of irradiation
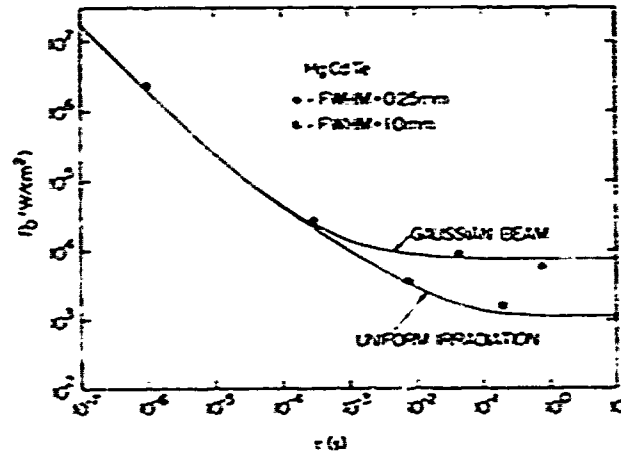time for two beam diameters

Fig. 4 — Power-density damage thresholds for
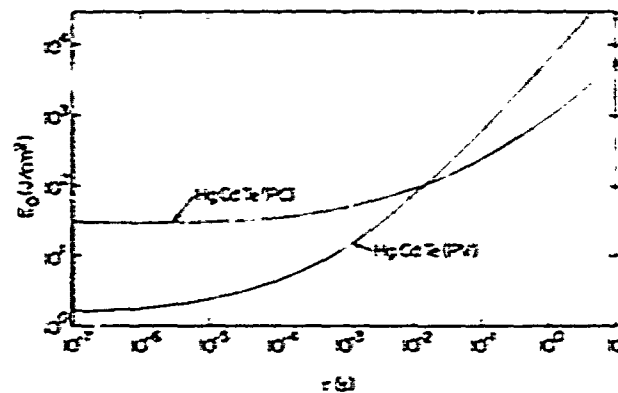HgCdTe crystals as a function of irradiation
time for two beam diameters

Fig. 5 — Comparison of calculated energy-density damage thresholds for HgCdTe (PV) and HgCdTe (PC) detectors
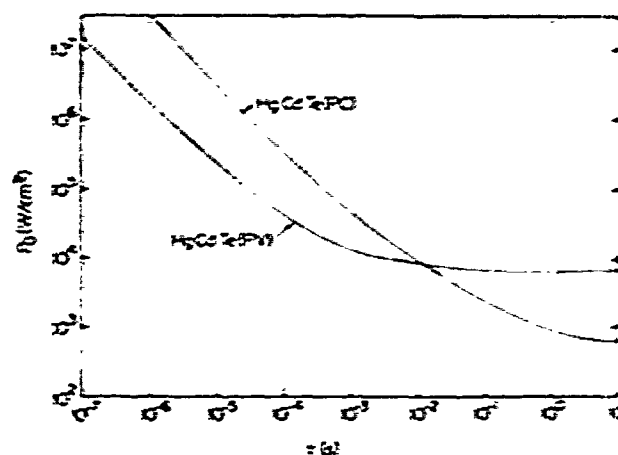

Fig. 6 — Comparison of calculated power-density damage thresholds for HgCdTe (PV) and HgCdTe (PC) detectors

In Figs. 5 and 6 the theoretical damage thresholds for HgCdTe photovoltaic and photoconductive (PC) detectors [1] are compared. Note that in the short-time limit the threshold for the photoconductor is more than an order of magnitude greater than for the photovoltaic detector. This is due mainly to the extra energy required to vaporize the larger active volume of the photoconductor. For intermediate times the thresholds approach each other since at these times the energy removed by heat conduction is large compared to the

S

energy required to vaporize the photoconductor. For the long-time limit ($\tau > 10^{-1}$s) the photovoltaic detector is more difficult to damage than the photoconductor. This is due to the importance of radial heat conduction at long irradiation times for HgCdTe (PV). Due to its construction, the photovoltaic detector is more effective at conducting heat away from the absorbing region. This arises both from the absence of any thermally resistive layers in the photovoltaic construction and from the lack of any significant radial heat conduction in a similarly irradiated photoconductor*.

Calculated threshold values of energy density are plotted in Fig. 7 as a function of irradiation time for various beam diameters in the range 0.05 mm $\leq$ FWHM $\leq$ 0.50 mm. As expected, all curves are approximately equal in the short-time limit, where thermal conduction has a negligible effect on the damage threshold. In the long-time limit, however, the damage threshold depends strongly on beam diameter, and E_0 is approximately inversely proportional to the beam diameter (Fig. 7). This dependence on beam diameter continues until the beam diameter becomes comparable to the detector thickness.
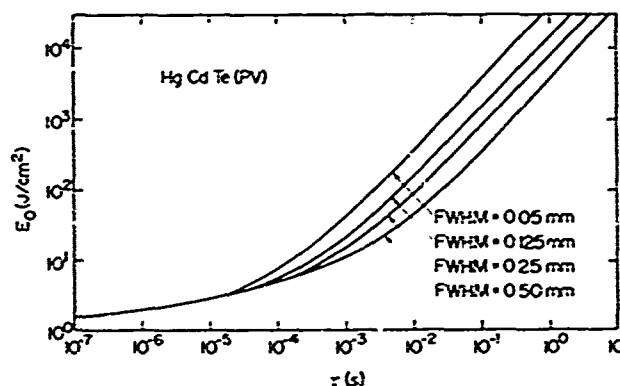

Fig. 7 — Calculated energy-density damage thresholds
for HgCdTe (PV) for various beam diameters

It is interesting to compare the calculated damage thresholds for HgCdTe (PV) to those obtained for PbSnTe (PV) [1]. In both cases it is assumed that the laser beam full width at half maximum was equal to the width of the active detector element (FWHM = 0.25 mm). From Figs. 8 and 9 we observe that the damage thresholds for both detectors are approximately equal for short irradiation times ($\tau < 10^{-4}$ s). As the irradiation time increases, the damage thresholds for HgCdTe PV detectors grow larger than those for PbSnTe PV detectors by an increasing margin.

---

* Damage thresholds for HgCdTe PC detectors were calculated in Ref. 1 using a model which assumes one-dimensional heat flow. To validate this model, thresholds were measured for HgCdTe samples mounted on substrates of approximately the same cross-sectional area. If the HgCdTe PC samples were placed on large-area substrates, radial heat conduction would again be important at long irradiation times.
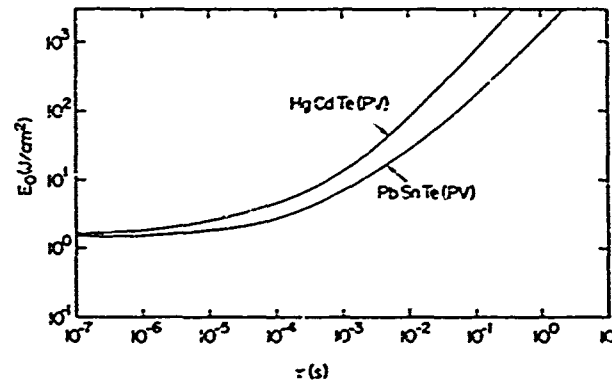
Fig. 8 — Comparison of calculated energy-density damage
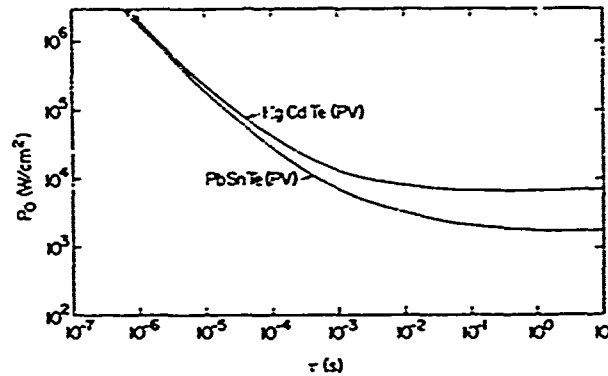thresholds for HgCdTe (PV) and PbSnTe (PV) detectors

Fig. 9 — Comparison of calculated power-density damage
thresholds for HgCdTe (PV) and PbSnTe (PV) detectors

It can be shown that the difference between the damage thresholds calculated for these
detectors is due to more efficient radial heat conduction for the HgCdTe PV detector. In the
long-time limit the damage threshold varies linearly with thermal conductivity. Since the thermal conductivity of HgCdTe is four times greater than that for PbSnTe, it is concluded that
the difference between the damage thresholds for these two detectors is due primarily to their
different thermal conductivities. This is so because the critical temperature change was found
empirically to be very close for these materials ($660°K$ and $733°K$ for HgCdTe and PbSnTe
respectively).

SUMMARY

Over the range of irradiation times studied (10^{-6}s to 1s), threshold values of E_0 and P_0 changed by three to four orders of magnitude. Significant differences were obtained between damage thresholds for samples irradiated by a Gaussian beam whose area is small compared to the crystal area and the thresholds for uniformly irradiated samples.

A two-dimensional thermal model employing numerical techniques was applied to HgCdTe PV detector materials, and good agreement was found between the theory and experimental results. This model takes into account all relevant details of detector geometry and thermal configuration and is capable of treating the cases of uniform and small Gaussian beam irradiation of the detectors. Such a model is required if damage thresholds are to be calculated for these detectors for all possible irradiation conditions.

The calculated damage thresholds for HgCdTe PV detectors were compared to those for HgCdTe PC and PbSnTe PV detectors. It was found that for short irradiation times, HgCdTe photoconductors are significantly more difficult to damage because of the large amount of energy required to vaporize the entire photoconductive detector. For long times ($\tau > 10^{-2}$s) the HgCdTe photovoltaic detector is more difficult to damage because of the importance of radial heat conduction in this detector. The damage thresholds for HgCdTe PV and PbSnTe PV detectors are approximately equal for short times but at long times HgCdTe (PV) is more difficult to damage primarily because its thermal conductivity is greater than that of PbSnTe.

REFERENCES

1. F. Bartoli, L. Esterowitz, M. Kruer, and R. Allen, "Thermal modeling of laser damage in 8-14-μm HgCdTe photoconductive and PbSnTe photovoltaic detectors," J. Appl. Phys. 46, No. 10, 4519 (1975).

2. M. R. Kruer, L. Esterowitz, F.J. Bartoli, and R.E. Allen, "Optical radiation damage of SBN materials and pyroelectric detectors at 10.6 μm, J. Appl. Phys. 46, No. 3, 1072 (1975).

3. P.J. Torvik, "A Numerical Procedure for Two-Dimensional Heating and Melting Calculations tions with Application to Laser Effects," Technical Report AFIT TR 72-2, Air Force Institute of Technology, March 1972.